Identifiability Analysis of Oversampled Uniform Linear Arrays Under Practical Considerations

Md. Waqeeb T. S. Chowdhury [†], Yimin D. Zhang [†], and Braham Himed [‡]

[†] Department of Electrical and Computer Engineering, Temple University, Philadelphia, PA 19122, USA
[‡] Passive RF Systems Branch, Air Force Research Laboratory, WPAFB, OH 45433, USA

***Abstract*—In this paper, we analyze the identifiability of spatially oversampled uniform linear arrays (ULAs) under practical constraints including finite snapshots, noise, and mutual coupling. For a fixed aperture, spatial oversampling increases the number of sensors and thus the degrees-of-freedom compared with integer ULAs. We show that the eigenvalues of the sample covariance matrix deviate from those of the true covariance matrix, with the smallest eigenvalue consistently underestimated and converging to the true value only as the number of snapshots increases. Assuming an equal number of sources and sensors, we examine how the smallest eigenvalue of the estimated sample covariance matrix behaves relative to the noise power, comparing scenarios with and without mutual coupling for both integer and oversampled ULAs. To examine the role of mutual coupling, we extend the existing mutual coupling model developed for integer arrays to a general distance-aware model suitable for oversampled ULAs. Simulation results demonstrate that oversampled ULAs are highly sensitive to mutual coupling, requiring a higher signal-to-noise ratio to retain identifiability.**

Keywords: Oversampled uniform linear array, mutual coupling, covariance estimation, identifiability, smallest eigenvalue.

I. Introduction

Estimating the direction of arrival (DOA) of signals using sensor arrays is a fundamental problem in array signal processing and has been extensively studied over several decades [1, 2]. Uniform linear arrays (ULAs) are widely used in array processing due to their simple structure and well-characterized performance. For an N-element ULA with half-wavelength inter-element spacing, it is well established that the array provides $N-1$ degrees-of-freedom (DOFs), which determine its ability to resolve distinct sources. To extend this limit, various array geometries and processing techniques have been proposed, including sparse arrays [3–9] and multi-frequency extensions [10–12] that increase the spatial DOFs exploiting time and frequency resources. It is important to note that these designs, whether ULAs, sparse arrays, or multi-frequency extensions, are generally based on the assumption of half wavelength unit spacing.

More recently, researchers have explored array structures that relax the conventional half-wavelength spacing assumption. Non-integer and rational arrays, for example, adjust sensor positions or exploit rational frequency relationships to improve resolvability [13–19]. Oversampled ULAs address this challenge by increasing sensor density within a fixed aperture, thereby reducing inter-element spacing. These studies provide valuable insights into increasing the nominal number of DOFs and improving identifiability within a limited array aperture by adjusting the inter-element spacing. However, most existing reports rely on idealized assumptions, and their robustness under practical conditions remains unclear.

In practice, array performance is affected by noise, limited number of snapshots, and mutual coupling between closely spaced sensors. These factors distort the sample covariance matrix and alter the behavior of its eigenvalues, which underlie subspace-based DOA estimation methods. In particular, the smallest signal-subspace eigenvalue is critical for separating the signal and noise subspaces, and its sensitivity to perturbations directly impacts the array identifiability. While spatial oversampling increases the nominal DOFs, the reduced inter-element spacing also makes oversampled arrays more susceptible to the effects of mutual coupling and finite-sample errors.

This paper examines the identifiability of oversampled ULAs under practical impairments. We investigate how noise, a limited number of snapshots, and mutual coupling affect the smallest signal-subspace eigenvalue of the sample covariance matrix and its ability to separate the signal and noise subspaces. We present analytical insights using perturbation theory to show how a finite number of snapshots introduces a systematic bias in the smallest signal-subspace eigenvalue, followed by validation using simulation results. The results highlight a clear tradeoff: While oversampled ULAs offer more nominal DOFs than conventional arrays, they are considerably more sensitive to practical impairments and demand higher signal-to-noise ratios (SNR) to maintain identifiability.

Notations: We use lower-case and upper-case bold characters to denote vectors and matrices, respectively. In particular, $\mathbf{I}_N$ denotes the $N\times N$ identity matrix and $\mathbf{0}$ stands for a vector or matrix of all zeros with a proper dimension. $(\cdot)^{\mathrm{T}}$, $(\cdot)^{\mathrm{H}}$, and $\mathbb{E}[\cdot]$ denote transpose, Hermitian, and expectation. $\mathrm{diag}(\cdot)$ forms a diagonal matrix. The (m,n)th entry of a matrix $\boldsymbol{B}$ is given by $[\boldsymbol{B}]_{m,n}$. Finally, $\mathbb{C}^{M\times N}$ denotes the $M\times N$ complex space.

This material is based upon work supported by the Air Force Office of Scientific Research under award number FA9550-23-1-0255. Any opinions, findings, and conclusions or recommendations expressed in this material are those of the authors and do not necessarily reflect the views of the United States Air Force.

II. System Model

In this section, we develop the system model used throughout the paper. We first present the signal model and mutual coupling formulation for a ULA with half-wavelength inter-element spacing in Subsection II-A. This baseline model is then extended to spatially oversampled ULAs in Subsection II-B, where the array aperture is kept fixed while the inter-element spacing is compressed. Although the signal model remains unchanged, the mutual coupling formulation is modified to account for the reduced spacing.

A. Signal and Mutual Coupling Model for Integer ULAs

We start with considering an N-element ULA with inter-element spacing $d = \lambda/2$, with λ denoting the wavelength. ULAs with half-wavelength spacing are referred to as integer arrays. Let L uncorrelated sources impinge on the array with distinct DOAs $\theta_1, \theta_2, \cdots, \theta_L$. The steering vector of the array corresponding to the source at direction θ_l is given as

$$\boldsymbol{a}(\theta_l) = \left[1,\ e^{-\jmath 2\pi \frac{d}{\lambda}\sin(\theta_l)}, \cdots,\ e^{-\jmath 2\pi (N-1)\frac{d}{\lambda}\sin(\theta_l)}\right]^{\mathrm{T}}. \quad (1)$$

The $N \times 1$ signal vector received by the ULA corresponding to all L sources is expressed as

$$\boldsymbol{x}(t) = \sum_{l=1}^{L} \boldsymbol{a}(\theta_l) s_l(t) + \boldsymbol{n}(t) = \boldsymbol{A}\boldsymbol{s}(t) + \boldsymbol{n}(t), \quad (2)$$

where $\boldsymbol{A} = [\boldsymbol{a}(\theta_1), \boldsymbol{a}(\theta_2), \cdots, \boldsymbol{a}(\theta_L)]$ is the array manifold of the ULA and $\boldsymbol{s}(t) = [s_1(t), s_2(t), \cdots, s_L(t)]^{\mathrm{T}}$ is the source signal vector. Moreover, $\boldsymbol{n}(t) \sim \mathcal{CN}(\boldsymbol{0}, \sigma_n^2 \mathbf{I}_N)$ denotes the additive zero-mean circularly complex white Gaussian noise vector observed at the ULA. The covariance matrix of the received signal vector $\boldsymbol{x}(t)$ assuming perfect statistics is given as

$$\boldsymbol{R}_x = \mathbb{E}\left[\boldsymbol{x}(t)\boldsymbol{x}^{\mathrm{H}}(t)\right] = \boldsymbol{A}\boldsymbol{R}_s\boldsymbol{A}^{\mathrm{H}} + \sigma_n^2 \boldsymbol{I}_N. \quad (3)$$

In practice, where perfect statistical conditions are not met, the sample covariance matrix is estimated using T snapshots of the received data vector $\boldsymbol{x}(t)$ as

$$\hat{\boldsymbol{R}}_x = \frac{1}{T}\sum_{t=1}^{T} \boldsymbol{x}(t)\boldsymbol{x}^{\mathrm{H}}(t). \quad (4)$$

Another important factor to be considered in practice is mutual coupling between the physical sensors. Mutual coupling distorts the received signals due to electromagnetic interactions between antenna elements, leading to model mismatches. This effect can be captured by introducing a coupling matrix $\boldsymbol{C} \in \mathbb{C}^{N\times N}$, which modifies the signal model in (2) as

$$\boldsymbol{x}(t) = \boldsymbol{C}\boldsymbol{A}\boldsymbol{s}(t) + \boldsymbol{n}(t), \quad (5)$$

and the covariance matrix in (3) becomes

$$\boldsymbol{R}_x = \boldsymbol{C}\boldsymbol{A}\boldsymbol{R}_s\boldsymbol{A}^{\mathrm{H}}\boldsymbol{C}^{\mathrm{H}} + \sigma_n^2 \boldsymbol{I}_n. \quad (6)$$

For the case of ULAs, the coupling matrix $\boldsymbol{C}$ is often modeled as a banded Toeplitz matrix, reflecting the fact that mutual coupling depends only on the relative spacing between antenna elements [20, 21]. Specifically, the Toeplitz structure arises from the translational invariance of the array geometry, where mutual coupling between two elements is determined solely by their separation. The main diagonal of $\boldsymbol{C}$ represents the self-response of each element and is typically considered as unity, while the off-diagonals capture the mutual coupling effect between neighboring sensors. Since electromagnetic interactions are primarily confined to sensors within a fixed physical separation, the coupling is typically modeled as significant only within this range, thereby giving rise to an R-banded Toeplitz structure for $\boldsymbol{C}$ with $R \leq N$ as

$$[\boldsymbol{C}]_{m,n} = \begin{cases} 1, & m = n, \\ c_r, & r = |m-n| \leq R, \\ 0, & \text{otherwise}, \end{cases} \quad (7)$$

where $m, n \in [0,\ 1,\ \cdots,\ N-1]$, and $c_0,\ c_1,\ \cdots,\ c_R$ are the coupling coefficients such that $1 = c_0 > |c_1| > |c_2| > \cdots > |c_R|$. A generalized form of the coupling coefficient c_r for $r = 1,\ 2, \ldots, R$ can be given as

$$c_r = c_1 \cdot f(r) \cdot e^{\jmath\phi_r}, \quad (8)$$

where c_1 represents the coupling coefficient at half-wavelength spacing, $f(r)$ models the coupling decay as a non-increasing function of sensor spacing, and $e^{\jmath\phi_r}$ represents the coupling phase.

In this paper, we adopt a banded mutual coupling coefficient model as [22, 23]

$$c_r = \frac{1}{r} c_1 e^{-\jmath(r-1)\frac{\pi}{8}}, \quad 1 < r \leq R, \quad (9)$$

where $c_1 = 0.3e^{\jmath\frac{\pi}{3}}$. It is noted that in this model $f(r) = 1/r$ and $\phi_r = -(r-1)\pi/8$.

B. Mutual Coupling Model for Oversampled ULAs

To analyze the effect of compressed inter-element spacing, we consider an N-element integer ULA with aperture $D = (N-1)d$ as the baseline, and oversample it by a factor of $\alpha \geq 1$ while keeping the aperture fixed. While the oversampling factor α can be either an integer or a fractional number, for analytical convenience, it is chosen such that $\tilde{N}$ is an integer. This results in an oversampled ULA with $\tilde{N} = \alpha(N-1)+1$ elements and a reduced inter-element spacing of $\tilde{d} = d/\alpha$. Therefore, the physical separation between two sensors indexed by m and n is given by $\delta_{m,n} = |m-n|\tilde{d} = rd/\alpha$, where $r = |m-n|$.

To capture the effect of spatial oversampling, the coupling model in (9) is adjusted by scaling the coefficients to reflect the compressed inter-element spacing, resulting in

$$c_r^{(\alpha)} = \frac{d}{\delta_{m,n}} c_1 e^{-\jmath\left(\frac{\delta_{m,n}}{d}-1\right)\frac{\pi}{8}} = \frac{\alpha}{r} c_1 e^{-\jmath\left(\frac{r}{\alpha}-1\right)\frac{\pi}{8}}, \quad (10)$$

where we used the superscript (α) to emphasize the oversampling factor.

III. Minimum Eigenvalue-Based Identifiability Analysis

The covariance matrix $\boldsymbol{R}_x$ can be expressed through eigen-decomposition as

$$\boldsymbol{R}_x = \boldsymbol{U}\boldsymbol{\Lambda}\boldsymbol{U}^{\mathrm{H}} = \sum_{p=1}^{L} \lambda_p \boldsymbol{u}_p \boldsymbol{u}_p^{\mathrm{H}} + \sum_{q=L+1}^{\tilde{N}} \lambda_q \boldsymbol{u}_q \boldsymbol{u}_q^{\mathrm{H}}, \tag{11}$$

where $\boldsymbol{U} = [\boldsymbol{u}_1, \boldsymbol{u}_2, \cdots, \boldsymbol{u}_{\tilde{N}}]$ contains all the eigenvectors and $\boldsymbol{\Lambda} = \mathrm{diag}([\lambda_1, \lambda_2, \cdots, \lambda_{\tilde{N}}])$ denotes the diagonal matrix containing the corresponding eigenvalues. Under ideal statistical conditions, the eigenvalues of $\boldsymbol{R}_x$ satisfy $\lambda_1 \geq \lambda_2 \geq \cdots \geq \lambda_L > \lambda_{L+1} = \cdots = \lambda_{\tilde{N}} = \sigma_n^2$. However, in practical scenarios where these ideal conditions are not met, the estimated eigenvalues of $\hat{\boldsymbol{R}}_x$ are generally related as $\hat{\lambda}_1 \geq \hat{\lambda}_2 \geq \cdots \geq \hat{\lambda}_L \geq \hat{\lambda}_{L+1} \geq \cdots \geq \hat{\lambda}_{\tilde{N}}$.

Assume that the number of sources is equal to the number of sensors, i.e., $L = \tilde{N}$, and the eigenvalues are all distinct. The effect of limited snapshots on the eigenvalue of the sample covariance matrix $\hat{\boldsymbol{R}}_x$ is analyzed. Denote $\Delta\boldsymbol{R}_x$ as the perturbation due to inaccurate estimation of the sample covariance matrix $\hat{\boldsymbol{R}}_x$ using T snapshots, i.e.,

$$\boldsymbol{R}_x = \hat{\boldsymbol{R}}_x + \Delta\boldsymbol{R}_x = \frac{1}{T}\sum_{t=1}^{T} \boldsymbol{x}(t)\boldsymbol{x}^{\mathrm{H}}(t) + \Delta\boldsymbol{R}_x. \tag{12}$$

From the matrix perturbation theorem, when $T \gg \tilde{N}$ so that the perturbation is small, the nth eigenvalue of $\hat{\boldsymbol{R}}_x$ is related to that of $\boldsymbol{R}_x$ as [24, 25]

$$\hat{\lambda}_n = \lambda_n + \boldsymbol{u}_n^{\mathrm{H}} \Delta\boldsymbol{R}_x \boldsymbol{u}_n + \sum_{n \neq m} \frac{|\boldsymbol{u}_m^{\mathrm{H}} \Delta\boldsymbol{R}_x \boldsymbol{u}_n|^2}{\lambda_n - \lambda_m}. \tag{13}$$

Taking the expectation on both sides of (13) and noting the fact that the eigenvalues of $\boldsymbol{R}_x$ are deterministic and $\mathbb{E}[\Delta\boldsymbol{R}_x] = \boldsymbol{0}$ for small perturbations, we have $\mathbb{E}\left[\boldsymbol{u}_n^{\mathrm{H}} \Delta\boldsymbol{R}_x \boldsymbol{u}_n\right] = \boldsymbol{u}_n^{\mathrm{H}} \mathbb{E}[\Delta\boldsymbol{R}_x]\, \boldsymbol{u}_n = 0$, yielding

$$\mathbb{E}[\hat{\lambda}_n] = \lambda_n + \sum_{n \neq m} \frac{\mathbb{E}\left[|\boldsymbol{u}_m^{\mathrm{H}} \Delta\boldsymbol{R}_x \boldsymbol{u}_n|^2\right]}{\lambda_n - \lambda_m}. \tag{14}$$

It can be shown that the estimated eigenvalue $\hat{\lambda}_n$ is related to the true eigenvalue λ_n as (Theorem 4 of [26])

$$\mathbb{E}[\hat{\lambda}_n] = \lambda_n + \frac{1}{T}\sum_{n \neq m} \frac{\lambda_n \lambda_m}{\lambda_n - \lambda_m}. \tag{15}$$

Since we consider the case of $L = \tilde{N}$, we observe in (15) that for the smallest signal eigenvalue $\lambda_{\tilde{N}}$, $\lambda_{\tilde{N}} < \lambda_m$ is satisfied for any $m \neq \tilde{N}$ and, as a result, the denominator of the second term on the right-hand side of (15) is always negative. That is, in the statistical sense, $\mathbb{E}[\hat{\lambda}_{\tilde{N}}] < \lambda_{\tilde{N}}$, implying that the expected value of the smallest estimated eigenvalue is always smaller than the true smallest eigenvalue. As the number of snapshots T increases, the second term at the right-hand side of (15) becomes smaller and the estimated eigenvalue $\hat{\lambda}_n$ approaches the true eigenvalue λ_n.

The above analysis applies for arrays both with and without mutual coupling, since the effect of coupling is already incorporated into $\boldsymbol{R}_x$ as in (6). Prior studies on mutual coupling show that inter-element interactions reshape the covariance eigenstructure by increasing the correlation among the array outputs, thereby compressing the signal eigenspectrum [27–29]. Consistent with this picture, [30] reports that, in the presence of mutual coupling, the smallest signal eigenvalue is pulled toward the noise floor, particularly at tighter inter-element spacings, thereby shrinking the eigen-gap between the signal and noise subspace. A smaller gap degrades subspace stability and weakens identifiability under finite snapshots, increasing the likelihood of subspace leakage. In practice, this leads to slower convergence of eigenspace estimates and reduced robustness of subspace-based DOA estimation methods due to mutual coupling.

The smallest eigenvalue plays a crucial role in DOA estimation as it governs the separation between the signal and noise subspaces. When $L = \tilde{N}$ and the smallest (signal) eigenvalue λ_L approaches the noise power σ_n^2, the signal subspace eigenvalue leaks into the noise subspace, making the corresponding source undetectable. As this gap narrows, subspace separation becomes more difficult, especially with a limited number of snapshots, where downward bias of λ_L further increases subspace leakage and estimation errors. Hence, the smallest eigenvalue reflects both the theoretical identifiability limit and the practical resolution capability of the array.

IV. Simulation Results

In this section, we present simulation results to examine the effects of a finite number of snapshots, noise, and mutual coupling on the identifiability of oversampled ULAs. We analyze the variation of the smallest signal subspace eigenvalues of the sample covariance matrix $\hat{\boldsymbol{R}}_x$ with varying input SNR levels and snapshot counts. We also verify our findings using DOA estimation results. In our simulations, we adopt a coupling radius of $R = 3\lambda$, meaning that only sensors within three wavelength (six half-wavelength) spacing are considered to be coupled.

Fig. 1 shows the eigenvalue behavior of the sample covariance matrix $\hat{\boldsymbol{R}}_x$ as a function of input SNR for $T = 100,\ 300$ and 700 snapshots without considering the effects of mutual coupling. An $N = 10$ element integer ULA with aperture $D = 9$ half-wavelengths is considered as a baseline. In Fig. 1(a), the minimum eigenvalue is plotted for the integer ULA with $L = 10$ sources. Fig. 1(b) reports the smallest signal subspace eigenvalue of the oversampled ULA ($\alpha = 2$) with $L = 10$ sources. Finally, in Fig. 1(c) the minimum eigenvalue is shown for the oversampled ULA with $L = 19$ sources. In all scenarios considered in Fig. 1, the sources are uniformly distributed within $[-60^\circ, 60^\circ]$. The noise power is normalized to unity and the signal power is adjusted according to the input SNR. To account for statistical fluctuations, the smallest eigenvalues are computed over 100 independent Monte Carlo trials. The solid lines show the average across trials, while the

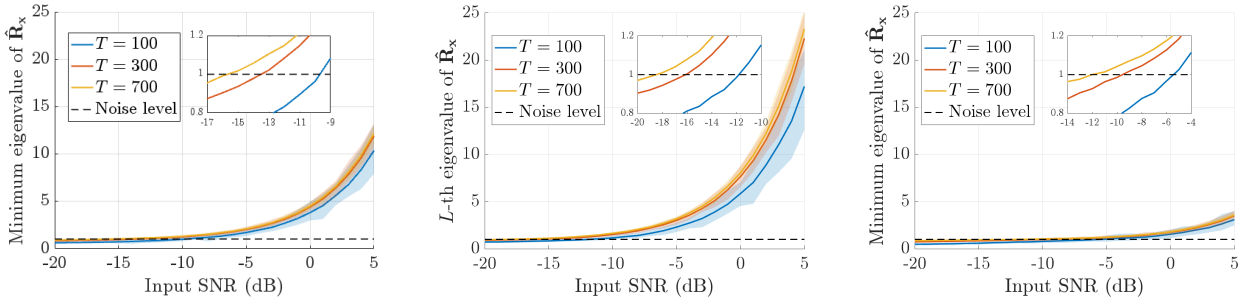

(a) $\alpha = 1$, $L = 10$ (b) $\alpha = 2$, $L = 10$ (c) $\alpha = 2$, $L = 19$

Fig. 1: Behavior of eigenvalues of $\hat{\boldsymbol{R}}_{\boldsymbol{x}}$ versus input SNR for different snapshot counts without mutual coupling. Each subfigure shows the minimum or Lth eigenvalue of $\hat{\boldsymbol{R}}_{\boldsymbol{x}}$ for different oversampling factors and signal configurations. 10-element integer ULA with $\alpha = 1$ and 19-element oversampled ULA with $\alpha = 2$ are considered.

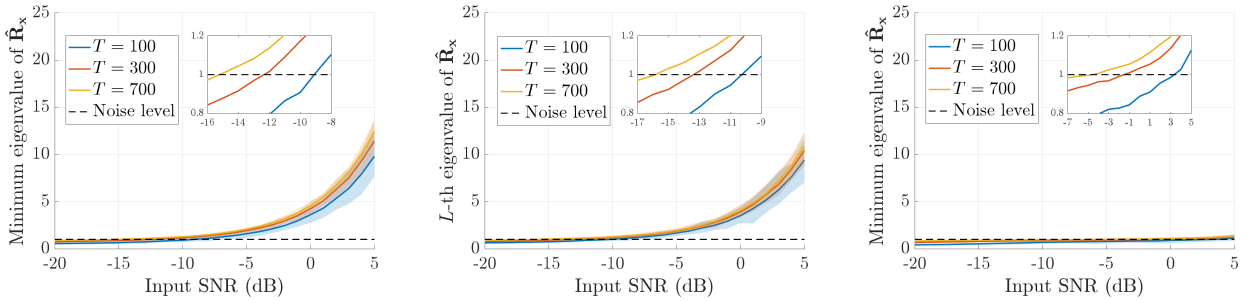

(a) $\alpha = 1$, $L = 10$ (b) $\alpha = 2$, $L = 10$ (c) $\alpha = 2$, $L = 19$

Fig. 2: Behavior of eigenvalues of $\hat{\boldsymbol{R}}_{\boldsymbol{x}}$ versus input SNR for different snapshot counts with mutual coupling. Each subfigure shows the minimum or Lth eigenvalue of $\hat{\boldsymbol{R}}_{\boldsymbol{x}}$ for different oversampling factors and signal configurations. 10-element integer ULA with $\alpha = 1$ and 19-element oversampled ULA with $\alpha = 2$ are considered.

shaded regions represent the spread (minimum to maximum), capturing variability due to finite-sample randomness.

In Fig. 1(a), corresponding to the integer ULA ($\alpha = 1$), the smallest eigenvalue remains above the noise floor only when the input SNR exceeds approximately -10 dB for $T = 100$. As the number of snapshots increases to $T = 300$ and $T = 700$, the eigenvalue stays consistently above the noise level at lower input SNR levels. It can be seen that for $T = 300$ the minimum eigenvalue is above the noise level for input SNR of -14 dB or higher, and for $T = 700$ the minimum input SNR requirement reduces to approximately -16 dB. This indicates that larger sample support stabilizes the covariance estimates and improves subspace separation.

In Fig. 1(b), for the oversampled ULA ($\alpha = 2$) with $L = 10$ sources, the required input SNR threshold reduces. For $T = 100$, the minimum signal subspace (or equivalently the Lth) eigenvalue exceeds the noise level when the input SNR is approximately above -12 dB, indicating that the eigenvalue is above the noise level for even smaller input SNR values since we have a larger number of sensors due to spatial oversampling. Similarly, the minimum SNR threshold at $T = 300$ and $T = 700$ decreases approximately to -16 dB and -18 dB, respectively. However, it is interesting to note that, in Fig. 1(c), for the oversampled ULA with $L = 19$ sources, the smallest eigenvalue is above the noise level for much higher input SNR values. The input SNR thresholds for $T = 100$, 300, and 700 cases are -5 dB, -10 dB, and -12 dB, respectively. Therefore, for a given number of sources, the smallest signal subspace eigenvalue remains above the noise level at much lower input SNRs for the oversampled ULA compared to the integer ULA. Moreover, with sufficiently high input SNR, the oversampled ULA can resolve significantly more sources than an integer ULA counterpart with a same aperture.

In Fig. 2, we included mutual coupling and the other setup is identical to that considered in Fig. 1. From Fig. 2(a), we see that the required input SNR thresholds increases compared to the thresholds shown in Fig. 1(a), since mutual coupling narrows the signal eigenspectrum and pushes the smallest eigenvalue toward the noise floor. Similar results are observed in Fig. 2(b), where the required minimum input SNR also becomes higher compared to that seen in Fig. 1(b). It is noted that the effect of mutual coupling is more severe in the oversampled ULA as the inter-element spacing is compressed, and the effect is more profound in the presence of a high number of sources. It can be seen in Fig. 2(c) for the $L = 19$ source case that the input SNR thresholds for $T = 100$, 300, and 700 cases become 3 dB, 0 dB, and -5 dB, respectively.

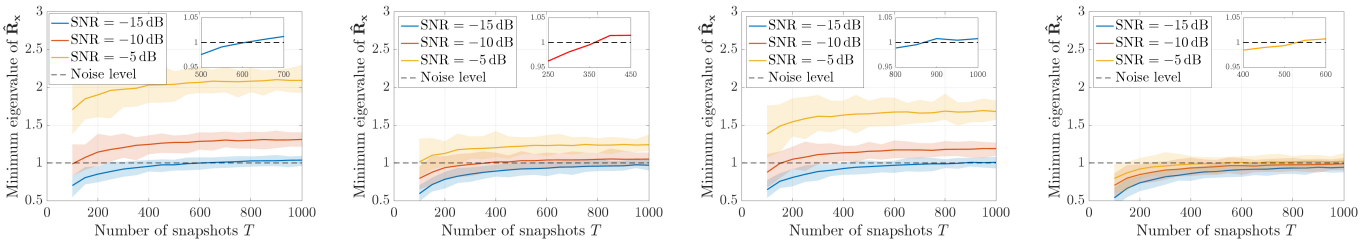

(a) $\alpha = 1$, $L = 10$, no coupling (b) $\alpha = 2$, $L = 19$, no coupling (c) $\alpha = 1$, $L = 10$, with coupling (d) $\alpha = 2$, $L = 19$, with coupling

Fig. 3: Smallest eigenvalue of $\hat{\boldsymbol{R}}_{\boldsymbol{x}}$ versus number of snapshots (T) for different input SNR levels, comparing cases with and without mutual coupling. 10-element integer ULA with $\alpha = 1$ and 19-element oversampled ULA with $\alpha = 2$ are considered.

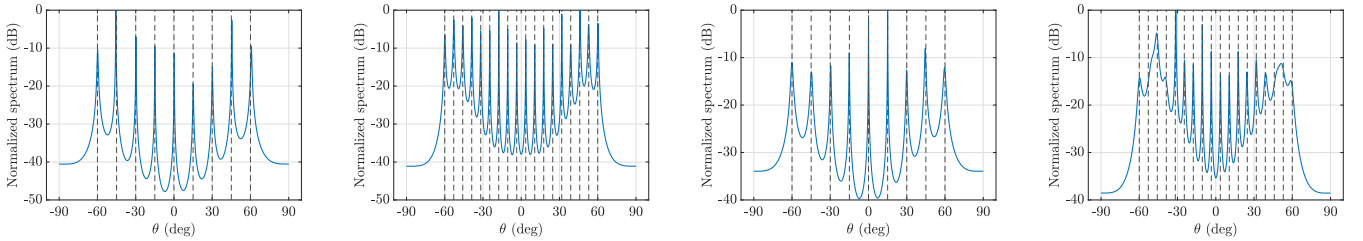

(a) $\alpha = 1$, no coupling: all 9 DOAs resolved (b) $\alpha = 2$, no coupling: all 18 DOAs resolved (c) $\alpha = 1$, with coupling: all 9 DOAs resolved (d) $\alpha = 2$, with coupling: all 18 DOAs not resolved

Fig. 4: MUSIC spectra illustrating the impact of oversampling and mutual coupling. 10-element integer ULA with $\alpha = 1$ and 19-element oversampled ULA with $\alpha = 2$ are considered.

Therefore, in comparison with Fig. 1(c), a much higher input SNR is needed in the presence of mutual coupling for the minimum eigenvalue to remain above the noise level. Provided a sufficient number of snapshots and higher signal power are available, the oversapled ULA can still resolve a higher number of sources compared to the integer ULA.

In Fig. 3, we examine the variation of the smallest eigenvalue of the sample covariance matrix $\hat{\boldsymbol{R}}_x$ as a function of the number of snapshots for different SNR values. From Fig. 3(a) we see that for the integer ULA, the smallest eigenvalue of $\hat{\boldsymbol{R}}_x$ remains above the noise level at SNR values of -5 and -10 dB even when the number of snapshots is small. But when SNR is equal to -15 dB, the minimum eigenvalue exceeds the noise level when $T = 600$ or larger. But in the presence of mutual coupling for the integer ULA, we see from Fig. 3(c) that, for the smallest eigenvalue to be above the noise level, we need a higher snapshot count of $T = 850$ or larger. However, from Fig. 3(b) and Fig. 3(d), we see that the impact of mutual coupling is far more severe in the oversampled ULA, where a much larger number of snapshots is needed to maintain the eigenvalue above the noise level at a given SNR. For the oversampled ULA with no mutual coupling, we can see that the smallest eigenvalue is consistently below the noise level for an input SNR of -15 dB. However, at an input SNR of -10 dB, we can see that the smallest eigenvalue exceeds the noise level for approximately $T = 400$ or larger. Comparing to the case with mutual coupling in Fig. 3(d), we see that in order to retain the minimum eigenvalue above the noise level, we need an input SNR of -5 dB, and sample support of at least $T = 500$. These results are consistent with Fig. 1 and Fig. 2 and show that, although oversampling increases the nominal degrees of freedom, it also makes the array more susceptible to degradation due to mutual coupling, which in turn reduces robustness at low SNR levels.

Fig. 4 presents the MUSIC spectra to examine how oversampling and mutual coupling affect DOA identifiability. The number of sources is set to one less than the number of sensors, with source directions uniformly distributed within $[-60°, 60°]$, using $T = 300$ snapshots and an SNR of 0 dB. As shown in Fig. 4(a), the integer ULA successfully resolves all 9 sources when no mutual coupling is considered. Fig. 4(b) illustrates that by increasing the oversampling factor to $\alpha = 2$, the number of virtual sensors increases to $\tilde{N} = 19$ within the same physical aperture, which allows resolution of all 18 sources with no mutual coupling. When mutual coupling is introduced, the performance difference between the two array configurations becomes more apparent. As seen in Fig. 4(c), the integer ULA still retains its ability to resolve all 9 sources despite the presence of coupling. In contrast, the oversampled array shown in Fig. 4(d) suffers from severe performance degradation, failing to resolve all 18 sources due to the increased sensitivity to mutual coupling. This performance degradation is attributed to the reduced inter-element spacing inherent in oversampled designs, which amplifies the effects of mutual coupling. Overall, while spatial oversampling enables higher nominal degrees of freedom and finer angular resolution, it also makes the array more vulnerable to distortions arising from mutual coupling and noise, particularly in dense array configurations.

V. Conclusion

This paper examined the identifiability of oversampled ULAs under practical constraints of finite snapshots, noise, and mutual coupling. By focusing on the behavior of the smallest eigenvalue of the sample covariance matrix, we highlighted how sample support and SNR jointly determine identifiability. With more snapshots, the estimated smallest eigenvalue reliably stays above the noise level even at low SNRs, while with fewer snapshots, stronger signals are needed to ensure identifiability. We also provide the relationship between the eigenvalues of the true covariance matrix and its estimate, showing that the smallest eigenvalue is systematically underestimated and converges to its true value as the number of snapshots increases. A distance-aware coupling model is proposed to assess the effect of mutual coupling in oversampled arrays. The results revealed that oversampled ULAs are more vulnerable to mutual coupling compared to integer ULAs, requiring stronger SNR conditions to preserve identifiability.

VI. References

[1] H. L. Van Trees, *Optimum Array Processing: Part IV of Detection, Estimation, and Modulation Theory*. Wiley, 2002.

[2] T. E. Tuncer and B. Friedlander (Eds.), *Classical and Modern Direction-of-Arrival Estimation*. Academic Press, 2009.

[3] P. Pal and P. P. Vaidyanathan, "Nested arrays: A novel approach to array processing with enhanced degrees of freedom," *IEEE Trans. Signal Process.*, vol. 58, no. 8, pp. 4167–4181, Aug. 2010.

[4] P. P. Vaidyanathan and P. Pal, "Sparse sensing with co-prime samplers and arrays," *IEEE Trans. Signal Process.*, vol. 59, no. 2, pp. 573–586, Feb. 2011.

[5] S. Qin, Y. D. Zhang, and M. G. Amin, "Generalized coprime array configurations for direction-of-arrival estimation," *IEEE Trans. Signal Process.*, vol. 63, no. 6, pp. 1377–1390, March 2015.

[6] A. Ahmed and Y. D. Zhang, "Generalized non-redundant sparse array designs," *IEEE Trans. Signal Process.*, vol. 69, pp. 4580–4594, Aug. 2021.

[7] Z. M. Liu, Z. T. Huang and Y. Y. Zhou, "Array signal processing via sparsity-inducing representation of the array covariance matrix," *IEEE Trans. Aerosp. Electron. Syst.*, vol. 49, no. 3, pp. 1710–1724, July 2013.

[8] C. Zhou, Y. Gu, X. Fan, Z. Shi, G. Mao, and Y. D. Zhang, "Direction-of-arrival estimation for coprime array via virtual array interpolation," *IEEE Trans. Signal Process.*, vol. 66, no. 22, pp. 5956–5971, Nov. 2018.

[9] N. Hu, Z. Ye, X. Xu and M. Bao, "DOA estimation for sparse array via sparse signal reconstruction," *IEEE Trans. Aerosp. Electron. Syst.*, vol. 49, no. 2, pp. 760-773, Apr. 2013.

[10] S. Qin, Y. D. Zhang, M. G. Amin, and B. Himed, "DOA estimation exploiting a uniform linear array with multiple co-prime frequencies," *Signal Process.*, vol. 130, pp. 37–46, Jan. 2017.

[11] A. Liu, X. Zhang, Q. Yang, and W. Deng, "Fast DOA estimation algorithms for sparse uniform linear array with multiple integer frequencies," *IEEE Access*, vol. 6, pp. 29952–29965, May 2018.

[12] S. Zhang, A. Ahmed, Y. D. Zhang, and S. Sun, "Enhanced DOA estimation exploiting multi-frequency sparse array," *IEEE Trans. Signal Process.*, vol. 69, pp. 5935–5946, Oct. 2021.

[13] Y. I. Abramovich, N. K. Spencer and A. Y. Gorokhov, "DOA estimation for noninteger linear antenna arrays with more uncorrelated sources than sensors," *IEEE Trans. Signal Process.*, vol. 48, no. 4, pp. 943–955, April 2000.

[14] Y. I. Abramovich and N. K. Spencer, "Design of nonuniform linear antenna array geometry and signal processing algorithm for DOA estimation of Gaussian sources," *Digital Signal Process.*, vol. 10, no. 4, pp. 340–354, Oct. 2000.

[15] P. Kulkarni and P. P. Vaidyanathan, "Non-integer arrays for array signal processing," *IEEE Trans. Signal Process.*, vol. 70, pp. 5457–5472, 2022.

[16] M. W. T. S. Chowdhury and Y. D. Zhang, "Unambiguous DOA estimation using multi-frequency rational sparse arrays," in *Proc. Asilomar Conf. Signals, Syst. Comput.*, Pacific Grove, CA, Oct. 2023, pp. 1324–1328.

[17] M. W. T. S. Chowdhury, Y. D. Zhang, W. Liu, and M. S. Greco, "Identifiability analysis of sensor arrays with sensors off half-wavelength grid," in *Proc. IEEE Int. Conf. Acoust., Speech, Signal Process. (ICASSP)*, Seoul, Korea, April 2024, pp. 8496–8500.

[18] M. W. T. S. Chowdhury, Y. D. Zhang and B. Himed, "Identifiability analysis of non-integer antenna arrays in the presence of mixed (strong and weak) signals," in *Proc. Int. Radar Conf.*, Rennes, France, Oct. 2024, pp. 1–6.

[19] M. W. T. S. Chowdhury and Y. D. Zhang, "Direction-of-arrival estimation exploiting oversampled uniform linear arrays," *IEEE Signal Process. Lett.*, in press.

[20] Z. Zheng, W. Wang, Y. Kong and Y. D. Zhang, "MISC array: A new sparse array design achieving increased degrees of freedom and reduced mutual coupling effect," *IEEE Trans. Signal Process.*, vol. 67, no. 7, pp. 1728–1741, April 2019.

[21] W. Shi, Y. Li and S. A. Vorobyov, "Low mutual coupling sparse array design using ULA fitting," in *Proc. IEEE Int. Conf. Acoust., Speech, Signal Process. (ICASSP)*, Toronto, ON, Canada, 2021, pp. 4610–4614.

[22] C. L. Liu and P. P. Vaidyanathan, "Super nested arrays: Linear sparse arrays with reduced mutual coupling–Part I: Fundamentals," *IEEE Trans. Signal Process.*, vol. 64, no. 15, pp. 3997–4012, Aug. 2016.

[23] J. Liu, Y. Zhang, Y. Lu, S. Ren, and S. Cao, "Augmented nested arrays with enhanced DOF and reduced mutual coupling," *IEEE Trans. Signal Process.*, vol. 65, no. 21, pp. 5549–5563, Nov. 2017.

[24] G. W. Stewart and J.-G. Sun, *Matrix Perturbation Theory*, Academic Press, 1990.

[25] B. Simon, "Fifty years of eigenvalue perturbation theory," *Bulletin American Math. Soc.*, vol. 24, no. 2, pp. 303–319, 1991.

[26] M. W. T. S. Chowdhury and Y. D. Zhang, "Identifiability analysis of non-integer antenna arrays," in preparation.

[27] B. Friedlander and A. J. Weiss, "Direction finding in the presence of mutual coupling," *IEEE Trans. Antennas Propag.*, vol. 39, no. 3, pp. 273–284, March 1991.

[28] H. Singh, H. L. Sneha, and R. M. Jha, "Mutual coupling in phased arrays: A review," *Int. J. Antennas Propag.*, vol. 2013, Art. ID 348123, 2013.

[29] B. Liao, Z.-G. Zhang, and S.-C. Chan, "DOA estimation and tracking of ULAs with mutual coupling," *IEEE Trans. Aerosp. Electron. Syst.*, vol. 48, no. 1, pp. 891–905, Jan. 2012.

[30] I. Gupta and A. Ksienski, "Effect of mutual coupling on the performance of adaptive arrays," *IEEE Trans. Antennas Propag.*, vol. 31, no. 5, pp. 785–791, Sept. 1983.